



# A Photoenzymatic NADH Regeneration System

Georg T. Höfler,<sup>[a]</sup> Elena Fernández-Fueyo,<sup>[a]</sup> Milja Pesic,<sup>[a]</sup> Sabry H. Younes,<sup>[a]</sup> Eun-Gyu Choi,<sup>[b]</sup> Yong H. Kim,<sup>[b]</sup> Vlada B. Urlacher,<sup>[c]</sup> Isabel W. C. E. Arends,<sup>[a]</sup> and Frank Hollmann<sup>\*[a]</sup>

A photoenzymatic NADH regeneration system was established. The combination of deazariboflavin as a photocatalyst with putidaredoxin reductase enabled the selective reduction of NAD<sup>+</sup> into the enzyme-active 1,4-NADH to promote an alcohol dehydrogenase catalysed stereospecific reduction reaction. The catalytic turnover of all the reaction components was demonstrated. Factors influencing the efficiency of the overall system were identified.

Biocatalytic redox reactions are receiving increasing attention in preparative organic synthesis.<sup>[1]</sup> Specifically, stereospecific ketoreductions and reductive aminations are now well established, especially in the pharmaceutical industry.<sup>[2]</sup> Being reductive by nature, these reactions need to be constantly supplied with reducing equivalents in the form of the reduced nicotinamide cofactors NAD(P)H. (Cost-)efficient reaction schemes inevitably involve sub-stoichiometric amounts of the NAD(P)H cofactors and their in situ regeneration.<sup>[3]</sup>

Having been stated decades ago,<sup>[4]</sup> it is not astonishing that a broad range of catalytic methods for the in situ regeneration of reduced nicotinamide cofactors have been developed.<sup>[3]</sup> All of them exhibit specific advantages and disadvantages, and it appears unlikely that a universal regeneration system will ever be found. In the 1970s, Willner and co-workers pioneered the use of visible light as a driving force to promote in situ NADPH regeneration.<sup>[5]</sup> Despite the promise of sunlight-driven cofactor regeneration, it was only in a few follow-up studies that this approach was further developed.<sup>[6]</sup> One reason is that photochemical redox reactions comprise single-electron-transfer

steps, which makes their direct application to NAD(P)<sup>+</sup> reduction impractical. This is due to the formation of enzyme-inactive NADH isomers and dimers.<sup>[7]</sup> A relay system to transform two successive single-electron steps into a (selective) hydride-transfer step is required. So far, the flavin adenine dinucleotide (FAD)-containing ferredoxin–NADP<sup>+</sup> reductase (FNR, E.C. 1.18.1.2) is the most widely used catalyst for this purpose.<sup>[8]</sup>

FNR, however, is highly selective for the phosphorylated nicotinamide cofactor (NADP<sup>+</sup>/NADPH) and is not applicable for the regeneration of the reduced, non-phosphorylated cofactor (NADH). We therefore evaluated the NAD-dependent putidaredoxin reductase (PDR) from *Pseudomonas putida* (E.C. 1.18.1.5)<sup>[9]</sup> as a relay system. Striving for simple reaction setups, we evaluated flavins as photocatalysts.<sup>[6,10]</sup> Overall, we aimed at establishing a photoenzymatic NADH regeneration system applicable to NADH-dependent, stereospecific reduction reactions (Scheme 1).

In a first set of experiments we evaluated some commercially available flavins as well as chemically synthesised deazariboflavin (dRf, details on the synthesis can be found in the Supporting Information) as photocatalysts to promote the reduction of NAD<sup>+</sup>. Significant NAD<sup>+</sup> reduction was observed only with dRf as the photocatalyst (Figure 1). Most likely, this can be attributed to the fact that the redox potential of the dRf/dRfH<sub>2</sub> couple (−0.273 V vs. standard hydrogen electrode, SHE) is more negative than that of flavin mononucleotide (FMN)/FMNH<sub>2</sub> or FAD/FADH<sub>2</sub> (−0.199 V vs. SHE),<sup>[11]</sup> which shifts the PDR redox equilibrium more to the reduced state. Strict exclusion of molecular oxygen from these reactions was crucial. Figure 1 compares the time courses of the photochemical NADH-formation reactions<sup>[12]</sup> under semi-anaerobic conditions (N<sub>2</sub> atmosphere, Figure 1A) and under glove box conditions (Figure 1B). Noteworthy, the apparent NADH concentration in the first case peaked after approximately 6 h, whereas steady NADH accumulation was observed under strict anaerobic conditions. Apparently, even a trace amount of molecular oxygen (entering the sample in the first case) irreversibly inhibits the photochemical NAD<sup>+</sup> reduction reaction.

Notably, in the absence of PDR, very significant reduction of NAD<sup>+</sup> (as judged spectrophotometrically) was also observed. This chemical reduction may be expected to yield significant amounts of non-enzyme-active NADH isomers such as 1,2-NADH, 1,6-NADH and/or NAD dimers (Scheme 2, photochemical),<sup>[13]</sup> whereas the PDR-mediated reduction of NAD<sup>+</sup> exclusively yields enzyme-active 1,4-NADH (Scheme 2, photoenzymatic).

Therefore, we further investigated the influence of the PDR concentration on the relative amount of 1,4-NADH formed (Figure 2). To assess the concentration of the latter, we used

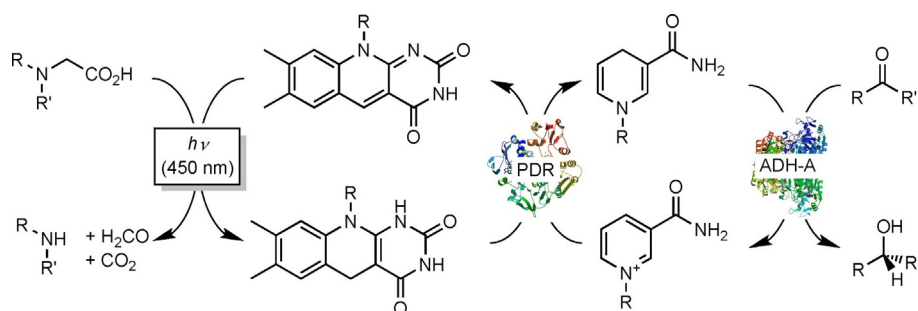
[a] G. T. Höfler, Dr. E. Fernández-Fueyo, Dr. M. Pesic, Dr. S. H. Younes, Prof. Dr. I. W. C. E. Arends, Dr. F. Hollmann  
Department of Biotechnology, Delft University of Technology  
van der Maasweg 9, 2629 HZ Delft (The Netherlands)  
E-mail: f.hollmann@tudelft.nl

[b] E.-G. Choi, Prof. Dr. Y. H. Kim  
School of Energy and Chemical Engineering  
Ulsan National Institute of Science and Technology  
Ulsan 689–798 (South Korea)

[c] Prof. Dr. V. B. Urlacher  
Chair of Biochemistry II, Heinrich Heine University Düsseldorf  
Universitätsstraße 1, 40225 Düsseldorf (Germany)

Supporting Information and the ORCID identification numbers for the authors of this article can be found under <https://doi.org/10.1002/cbic.201800530>.

© 2018 The Authors. Published by Wiley-VCH Verlag GmbH & Co. KGaA. This is an open access article under the terms of the Creative Commons Attribution Non-Commercial NoDerivs License, which permits use and distribution in any medium, provided the original work is properly cited, the use is non-commercial and no modifications or adaptations are made.



**Scheme 1.** Photoenzymatic reduction of  $\text{NAD}^+$  to promote alcohol dehydrogenase (ADH)-catalysed stereospecific reduction of ketones. A photocatalyst, deazariboflavin, promotes the light-driven oxidation of a sacrificial electron donor (e.g., ethylenediaminetetraacetic acid, EDTA) and delivers the reducing equivalents to the NADH-regeneration catalyst (putidaredoxin reductase, PDR). NADH is productively used by an alcohol dehydrogenase for the specific reduction of ketones to alcohols.

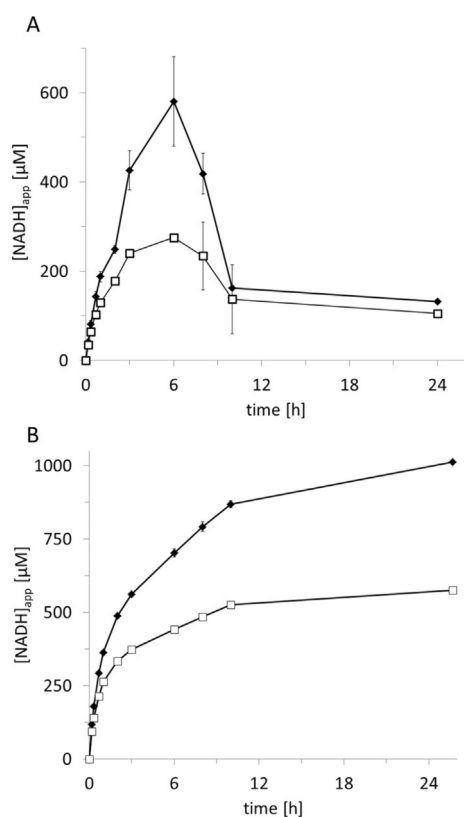


**Figure 1.** Photoenzymatic reduction of  $\text{NAD}^+$  in the presence (♦) and absence (□) of PDR. A) Results obtained under “anaerobic” conditions (using  $\text{N}_2$ -flushed reaction vessels under an otherwise ambient atmosphere). B) The same experiments performed entirely within a glove box. General conditions: 50 mM Tris-HCl buffer (pH 8),  $c(\text{NAD}^+) = 2 \text{ mM}$ ,  $c(\text{EDTA}) = 20 \text{ mM}$ ,  $c(\text{dRf}) = 60 \text{ }\mu\text{M}$ ,  $T = 30 \text{ }^\circ\text{C}$ ,  $\lambda = 450 \text{ nm}$ . Sampling: at intervals, samples were withdrawn, diluted in 50 mM Tris-HCl buffer (pH 8) and analysed spectrophotometrically. For calculation of the apparent NADH concentration, a molar extinction coefficient of  $6.22 \text{ M}^{-1} \text{ cm}^{-1}$  was used. Note that this method does not distinguish between 1,2-, 1,4-, 1,6-NADH, and NADH dimers. Exemplary UV/Vis spectra are shown in Figure S2.

a NADH-dependent ketoreduction reaction catalysed by the alcohol dehydrogenase (ADH) from *Rhodococcus ruber* (i.e., ADH-A; Figure 2).<sup>[14]</sup>

Quite expectedly, the use of a high molar surplus of the dRf photocatalyst resulted in poor selectivity of the  $\text{NAD}^+$  reduc-

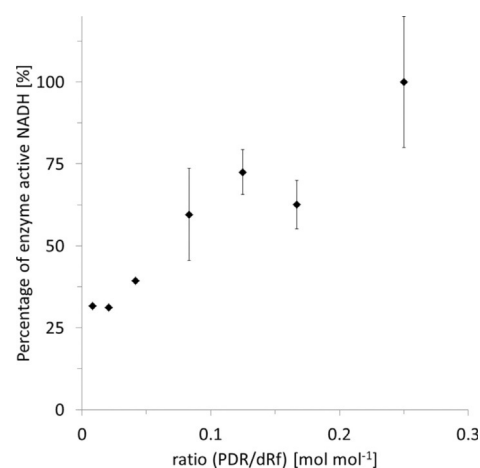
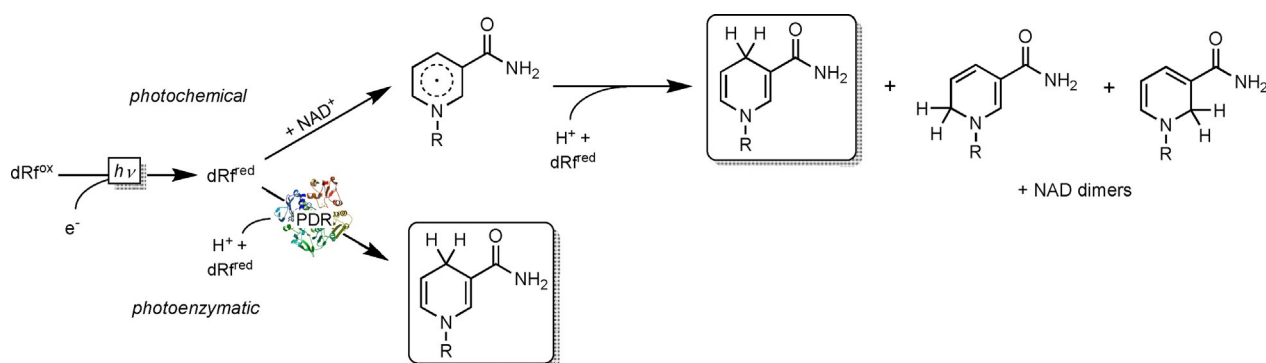


**Figure 2.** Influence of the dRf to PDR ratio on the selectivity of the photoenzymatic reduction of  $\text{NAD}^+$ . General conditions: the experiments were performed in a two-step, two-pot manner, that is, in a first step, the photoenzymatic reduction of  $\text{NAD}^+$  was conducted at varying concentrations of dRf and PDR. 50 mM Tris-HCl buffer (pH 8),  $c(\text{NAD}^+) = 2 \text{ mM}$ ,  $c(\text{EDTA}) = 20 \text{ mM}$ ,  $c(\text{ethyl acetoacetate}) = 10 \text{ mM}$ ,  $T = 30 \text{ }^\circ\text{C}$ ,  $\lambda = 450 \text{ nm}$ , semi-anaerobic. After 0.5–2.5 h, the reactions were stopped, the apparent NADH concentration was determined spectrophotometrically ( $\lambda = 340 \text{ nm}$ ) and the mixtures were supplemented with ADH-A (0.143  $\mu\text{M}$  final), incubated for 15 min and analysed by gas chromatography.

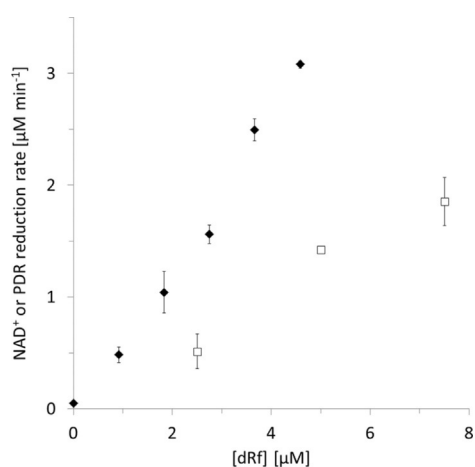
tion, and approximately one third of the overall reduced nicotinamide cofactor was the enzyme-active 1,4-NADH isomer. Nevertheless, at higher PDR concentrations, almost exclusive regioselectivity (i.e., fully enzymatic active NADH) was observed.

Further characterisation of the photoenzymatic  $\text{NAD}^+$  reduction system revealed that the overall rate (i.e., the rate of NADH formation) was largely independent of the PDR concentration applied (Figure S2 in the Supporting Information). The photocatalyst concentration, however, directly influenced the rate of the overall NADH generation reaction (Figure 3, □) and the rate of the PDR reduction (Figure 3, ♦).

Comparing both concentration dependencies, it becomes obvious that both were linearly dependent on the photocatalyst (dRf) concentration. The reduction of PDR was roughly two times faster than the overall  $\text{NAD}^+$  reduction, which suggested that the hydride-transfer rate from PDR-FADH<sub>2</sub> to  $\text{NAD}^+$  was



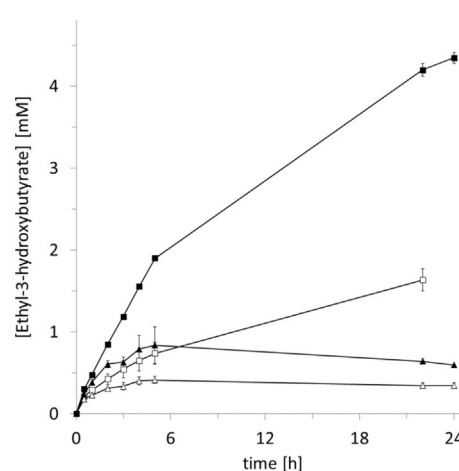
**Scheme 2.** Simplified representation of the two reactions competing for the photochemically formed, reduced deazariboflavin ( $\text{dRf}^{\text{red}}$ ).  $\text{dRf}^{\text{red}}$  undergoes direct electron transfer to  $\text{NAD}^+$  (photochemical reaction). The resulting NAD radical can either be protonated and reduced a second time leading to all NAD isomers possible or it can dimerise (for reasons of clarity, the different NAD dimers are not shown). Alternatively,  $\text{dRf}^{\text{red}}$  reduces PDR (as two successive single-electron-transfer reactions), which in its reduced form exclusively yields enzyme-active 1,4-NADH.



**Figure 3.** Rate dependency of the photoenzymatic reduction of  $\text{NAD}^+$  (□) and the PDR (◆) on the dRf concentration applied. General conditions: Tris-HCl buffer (50 mM, pH 8),  $c(\text{NAD}^+) = 0.4$  mM,  $c(\text{EDTA}) = 10$  mM,  $c(\text{PDR}) = 2.5$  (□) or 20 μM (◆),  $T = 25^\circ\text{C}$ ,  $\lambda = 450$  nm, anaerobic.

overall rate limiting. This is in line with the thermodynamically uphill character of this reaction. The reduction state of PDR (i.e.,  $[\text{PDR}^{\text{red}}]/[\text{PDR}^{\text{ox}}]$ ) is positively influenced by increasing in situ concentrations of  $\text{dRf}^{\text{red}}$ , which thereby also shifts the  $\text{NAD}^+/\text{NADH}$  equilibrium. This, however, may also come at the expense of an increased non-enzymatic reduction (i.e., non-selective reduction of  $\text{NAD}^+$ ).

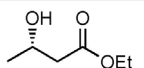
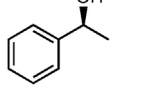
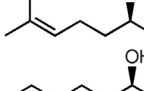
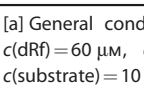
To assess the principal feasibility of the proposed photoenzymatic NADH regeneration scheme, we directly applied it to promote the ADH-A-catalysed reduction of ethyl acetoacetate in a one-pot, one-step reaction (Figure 4). Pleasingly, enantioselective reduction was feasible, and multiple turnovers for the nicotinamide cofactor were observed. Similar to the previous observation, a significant difference was observed between experiments performed under semi-anaerobic conditions (Figure 4, ▲ and △) and under strictly anaerobic conditions (i.e., in a glove box) (Figure 4, ■ and □). In the first case, product formation again ceased after approximately 5 h,<sup>[15]</sup> whereas in the latter case, more robust product accumulation for at least 24 h was observed.



**Figure 4.** Photoenzymatic reduction of ethyl acetoacetate to ethyl (*S*)-3-hydroxybutyrate by using the plain regeneration system (Scheme 1, open symbols) and in the presence of methyl viologen as a co-catalyst (closed symbols). Experiments were conducted under strictly anaerobic conditions (glove box, squares) or under semi-anaerobic reaction conditions ( $\text{N}_2$  atmosphere, triangles). General conditions: Tris-HCl buffer (50 mM, pH 8),  $c(\text{EDTA}) = 20$  mM,  $c(\text{dRf}) = 60$  μM,  $c(\text{NAD}^+) = 0.2$  mM,  $c(\text{PDR}) = 5$  μM,  $c(\text{ADH-A}) = 0.115$  μM,  $c(\text{ethyl acetoacetate}) = 10$  mM,  $T = 25^\circ\text{C}$ ,  $\lambda = 450$  nm, anaerobic;  $c(\text{MV}^{2+}) = 0$  (open symbols) or 0.25 mM (closed symbols).

In the past, methyl viologen ( $\text{MV}^{2+}$ ) has been used as a mediator for the ferredoxin- $\text{NADP}^+$ -reductase-catalysed regeneration of  $\text{NADPH}$ .<sup>[5,8d]</sup> We, therefore, also evaluated  $\text{MV}^{2+}$  in our reaction system (Figure 4, ■ and ▲). Notably, upon using  $\text{MV}^{2+}$  all catalytic components were also necessary to achieve reduction of ethyl acetoacetate. Performing the photoenzymatic reduction of ethyl acetoacetate in the presence of 0.25 mM  $\text{MV}^{2+}$  increased the product formation rate approximately three- to fourfold. Most probably,  $\text{MV}^{2+}$  served as a co-catalyst for the reduction of PDR and thereby favourably shifted its reduction state and shifted the  $\text{NADH}/\text{NAD}^+$  ratio. Unfortunately, spectrophotometric investigation of this hypothesis was not straightforward owing to the overlapping absorption spectra of PDR and  $\text{MV}^{2+}$ . Qualitatively, however, we observed electron transfer from  $\text{dRf}^{\text{red}}$  to  $\text{MV}^{2+}$  (Figure S3).

**Table 1.** Photoenzymatic reduction of various ketones.<sup>[a]</sup>

Product	without MV <sup>2+</sup>		with MV <sup>2+</sup>		c [mM] Control <sup>[b]</sup>
	c [mM]	ee [%]	c [mM]	ee [%]	
	0.86 ± 0.09	99	3.11 ± 0.07	99	8.47
	0.41 ± 0.01	99	1.6 ± 0.07	99	4.18
	0.21 ± 0.06	95	0.58 ± 0.15	96	2.86
	0.22 ± 0.05	99	0.65 ± 0.05	99	1.91

[a] General conditions: Tris-HCl buffer (50 mM, pH 8), c(EDTA) = 20 mM, c(dRf) = 60 μM, c(NAD<sup>+</sup>) = 0.2 mM, c(PDR) = 5 μM, c(ADH-A) = 0.115 μM, c(substrate) = 10 mM, T = 30 °C, t = 5 h, λ = 450 nm, semi-anaerobic, c(MV<sup>2+</sup>) = 0 or 0.25 mM. [b] Using NADH (10 mM) as a stoichiometric reductant.

The accelerating effect of MV<sup>2+</sup> was also observed during our preliminary exploration of the substrate scope of the photoenzymatic reduction system (Table 1). Pleasingly, the stereochemical outcome of the ADH-A-catalysed ketoreduction reaction was not impaired by the artificial regeneration system. This also excludes any direct reduction of the carbonyl starting materials by any other reactant. Up to 72, 21, 17, 868, and 37 700 turnovers were determined for dRf, NAD<sup>+</sup>, MV<sup>2+</sup>, PDR, and ADH-A, respectively.

Admittedly, relative to the productivity of the stoichiometric use of NADH, that of the current system falls back significantly. It should, however, be kept in mind that no efforts for optimising the photoenzymatic reaction system have so far been undertaken.

Especially, the robustness of the PDR under the current reaction conditions needs to be improved, as it was inactivated upon illumination with blue light (Figures S4 and S5). Most probably, the photoexcited enzyme-bound flavin cofactor is prone to photodegradation.<sup>[16]</sup> Hence, changing the photoexcitation wavelength appears to be of utmost importance to achieve robust photoenzymatic reaction schemes. Very promising preliminary results were obtained by changing the photocatalyst from dRf to safranin O (photoexcitation at λ = 519 nm, Figure S6), and continuous product formation for at least 5 days was shown.

Overall, with this contribution, we demonstrated that photoenzymatic regeneration of NADH was feasible by using the PDR from *Pseudomonas putida*. Potential pitfalls such as the undesired direct reduction of NAD<sup>+</sup> (leading to enzymatic-inactive NAD isomers) and the photodegradation of the flavin prosthetic group were identified together with some promising solutions. The next steps will concentrate at further opti-

misng the reaction setup to improve the NADH regeneration rate and therewith the practical feasibility of the approach.

## Acknowledgements

Financial support by the European Research Council (ERC Consolidator grant no.648026) is gratefully acknowledged.

## Conflict of Interest

The authors declare no conflict of interest.

**Keywords:** biocatalysis · enantioselectivity · ketones · photochemistry · reduction

- [1] U. T. Bornscheuer, G. W. Huisman, R. J. Kazlauskas, S. Lutz, J. C. Moore, K. Robins, *Nature* **2012**, *485*, 185–194.
- [2] a) G. W. Huisman, J. Liang, A. Krebber, *Curr. Opin. Chem. Biol.* **2010**, *14*, 122–129; b) W. Kroutil, H. Mang, K. Edegger, K. Faber, *Curr. Opin. Chem. Biol.* **2004**, *8*, 120–126.
- [3] a) A. Weckbecker, H. Gröger, W. Hummel, *Adv. Biochem. Eng./Biotechnol.* **2010**, *120*, 195–242; b) R. Wichmann, D. Vasic-Racki, *Adv. Biochem. Eng./Biotechnol.* **2005**, *92*, 225–260.
- [4] H. Chenault, G. Whitesides, *Appl. Biochem. Biotechnol.* **1987**, *14*, 147–197.
- [5] D. Mandler, I. Willner, *J. Chem. Soc. Perkin Trans. 2* **1986**, 805–811.
- [6] S. H. Lee, D. S. Choi, S. K. Kuk, C. B. Park, *Angew. Chem. Int. Ed.* **2018**, *57*, 7958–7985; *Angew. Chem.* **2018**, *130*, 8086–8116.
- [7] E. Steckhan, *Top. Curr. Chem.* **1994**, *170*, 83–111.
- [8] a) L. Wan, C. F. Megarity, B. Siritanaratkul, F. A. Armstrong, *Chem. Commun.* **2018**, *54*, 972–975; b) K. A. Brown, M. B. Wilker, M. Boehm, H. Hamby, G. Dukovic, P. W. King, *ACS Catal.* **2016**, *6*, 2201–2204; c) H. Asada, T. Itoh, Y. Kodera, A. Matsushima, M. Hiroto, H. Nishimura, Y. Inada, *Biotechnol. Bioeng.* **2001**, *76*, 86–90; d) J. J. Pueyo, C. Gomez-moruno, *Enz. Microb. Technol.* **1992**, *14*, 8–12.
- [9] I. F. Sevrioukova, T. L. Poulos, *J. Biol. Chem.* **2002**, *277*, 25831–25839.
- [10] a) W. Zhang, F. Hollmann, *Chem. Commun.* **2018**, *54*, 7281–7289; b) W. R. Frisell, C. W. Chung, C. G. Mackenzie, *J. Biol. Chem.* **1959**, *234*, 1297–1302.
- [11] M. T. Stankovich, V. Massey, *Biochim. Biophys. Acta Enzymol.* **1976**, *452*, 335–344.
- [12] Note that the apparent NADH concentration was estimated spectrophotometrically at 340 nm by using a molar extinction coefficient of 6.22 cm<sup>-1</sup> M<sup>-1</sup>. This method does not distinguish between enzymatically active 1,4-NADH and its (enzyme inactive) regioisomers.
- [13] a) H.-J. Duchstein, H. Fenner, P. Hemmerich, W.-R. Knappe, *Eur. J. Biochem.* **1979**, *95*, 167–181; b) W. R. Knappe, P. Hemmerich, H. J. Duchstein, H. Fenner, V. Massey, *Biochemistry* **1978**, *17*, 16–17.
- [14] a) B. Kosjek, W. Stampfer, M. Pogorevc, W. Goessler, K. Faber, W. Kroutil, *Biotechnol. Bioeng.* **2004**, *86*, 55–62; b) W. Stampfer, B. Kosjek, W. Kroutil, K. Faber, *Biotechnol. Bioeng.* **2003**, *81*, 865–869; c) W. Stampfer, B. Kosjek, K. Faber, W. Kroutil, *J. Org. Chem.* **2003**, *68*, 402–406; d) W. Stampfer, B. Kosjek, K. Faber, W. Kroutil, *Tetrahedron: Asymmetry* **2003**, *14*, 275–280.
- [15] The apparent small decrease in the product concentration is most likely due to hydrolysis of the ethyl ester product, which could not be determined with the GC method used.
- [16] W. Holzer, J. Shirdel, P. Zirak, A. Penzkofer, P. Hegemann, R. Deutzmann, E. Hochmuth, *Chem. Phys.* **2005**, *308*, 69–78.

Manuscript received: September 7, 2018

Accepted manuscript online: September 7, 2018

Version of record online: October 23, 2018